From Antimatter to Disease Detection: The Use of Radioisotopes in the Life Sciences

Part 2: PET radioisotopes

Suzanne Lapi, Ph.D

Assistant Professor

Department of Radiology,

Washington University

Mallinckrodt Institute of Radiology

Washington University in St. Louis School of Medicine

Types of Radioactive Decay

- α – emission of a He nucleus
- β^- – electron emission
- β^+ – positron emission
- γ – gamma emission

Therapy (α, β^-)

Imaging (β^+, γ)

Diagnostic medicine:
Look into the body to see what is happening

Rembrandt - anatomy lesion

How can we probe the human body without a knife?

Nuclear Imaging

SPECT: Single Photon Emission
Computed Tomography

PET: Positron Emission Tomography

Imaging with γ emitters

In planar imaging, the camera records an image from one perspective

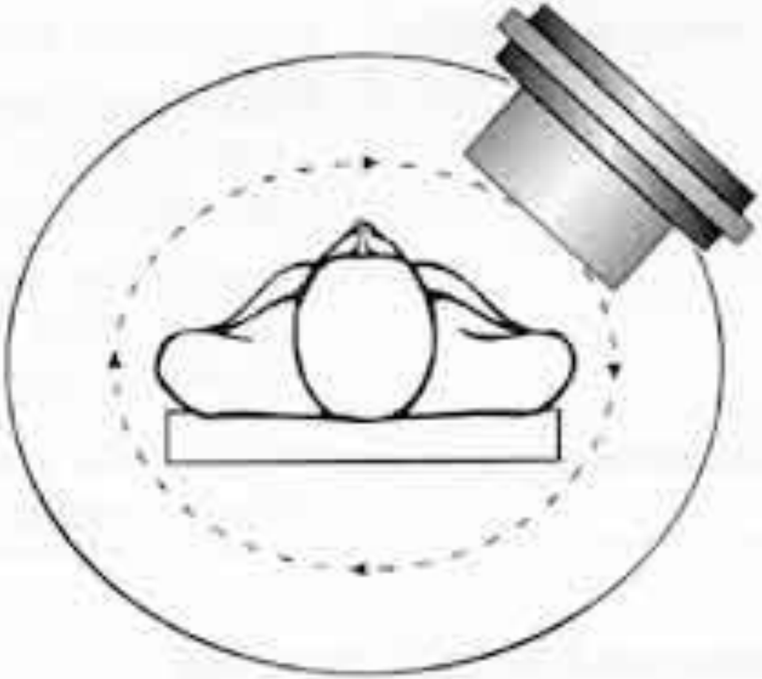

In SPECT imaging, the camera rotates around the patient, recording multiple images that are then reconstructed into a three-dimensional data set by a computer

Why Use PET Imaging?

- PET imaging is capable of providing quantitative information about biochemical and physiological processes, *in vivo*.

Basic Principles of Positron Emission Tomography (PET)

- Based on tracer principle.
- Tracer labeled with positron emitting radioisotope.
- Positron decay.
- Coincidence detection of annihilation radiation.

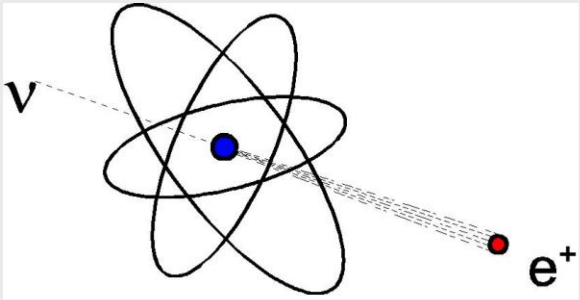
ν
e+

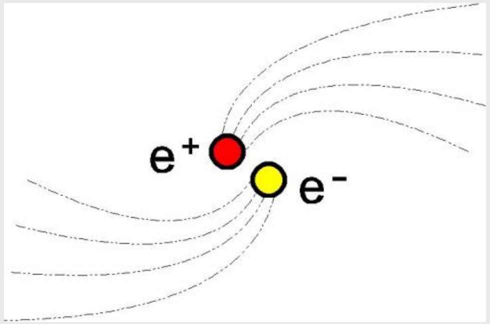
e+
e-

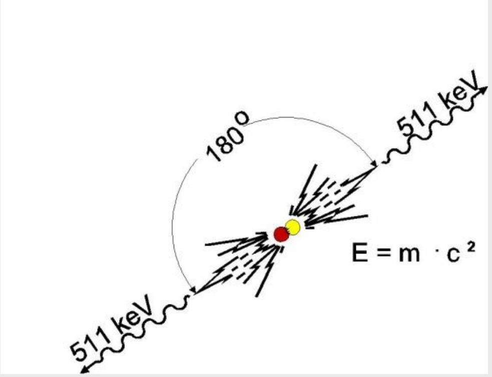
180°
511 keV
511 keV
E = m · c ²

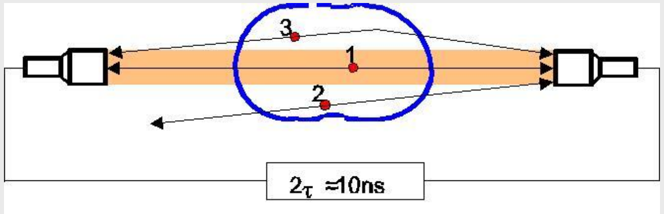
3
1
2
2τ ≈10ns

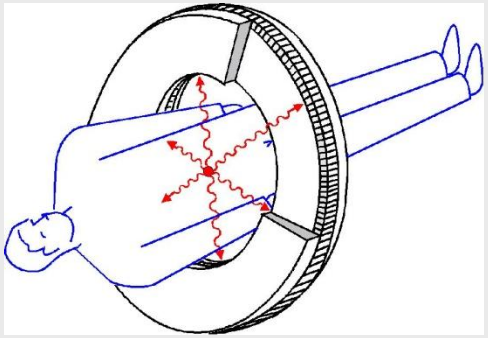

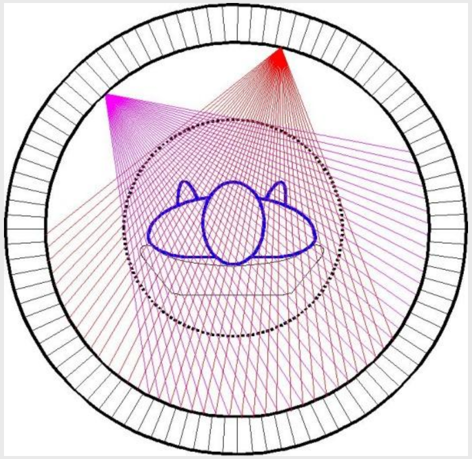

Principle of PET Imaging (1)

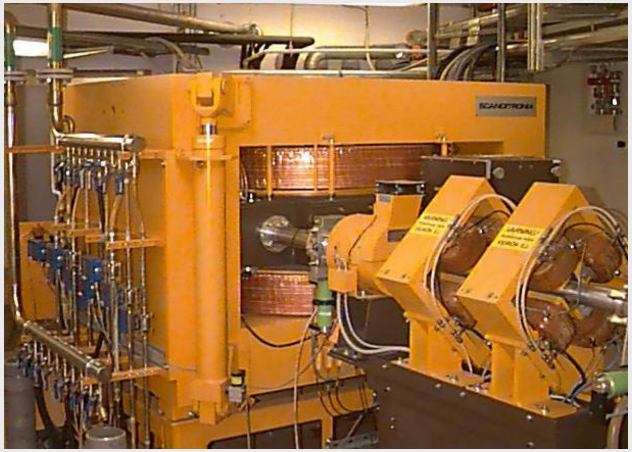

- ⇒ Positron-emitting isotopes produced on cyclotrons or generators
- ⇒ Injection of a tracer compound labeled with a positron-emitting radionuclide
- ⇒ The radionuclide in the radiotracer decays and the resulting positrons subsequently annihilate on contact with electrons after traveling a short distance (~ 1-10 mm) within the body

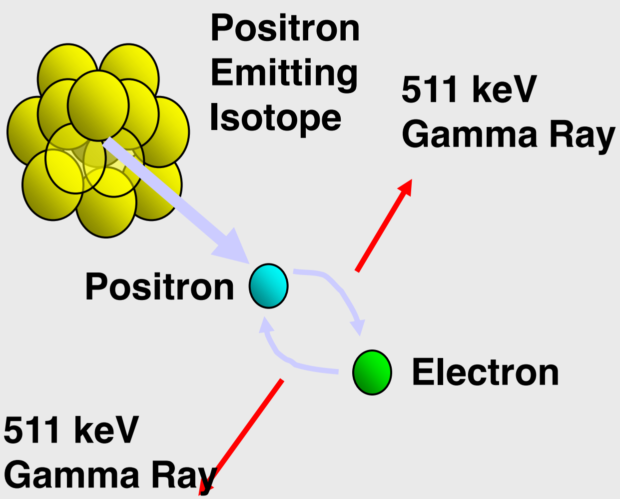

Principle of PET Imaging (2)

⇒ Each annihilation produces two 511 keV photons traveling in opposite directions (180^{O}) which are detected by the detectors surrounding the subject

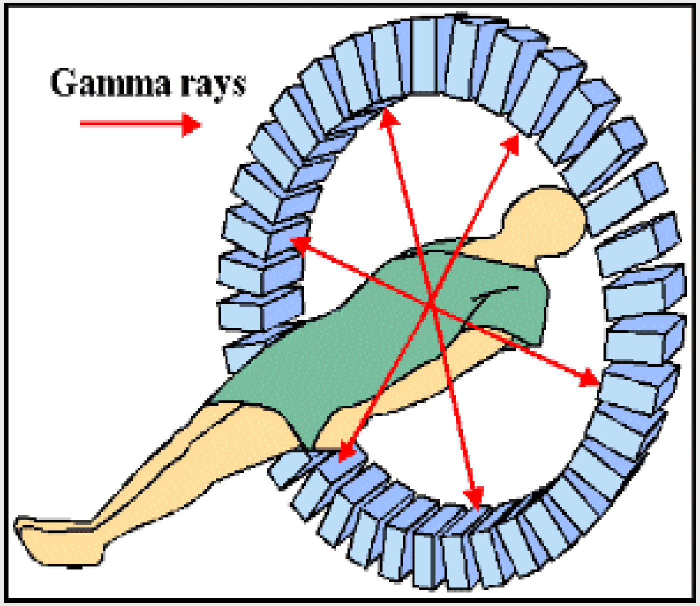

Early PET Imaging

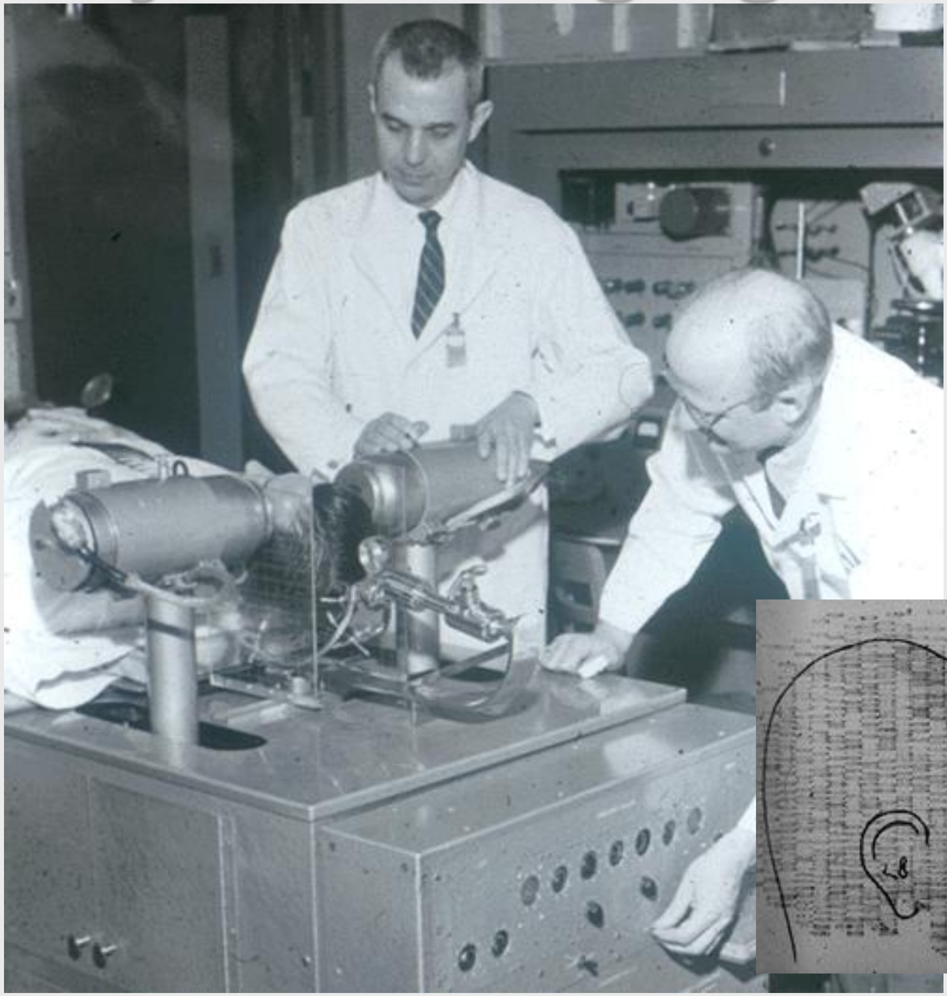

1951:

Gordon L. Brownell and colleagues at the Massachusetts General Hospital

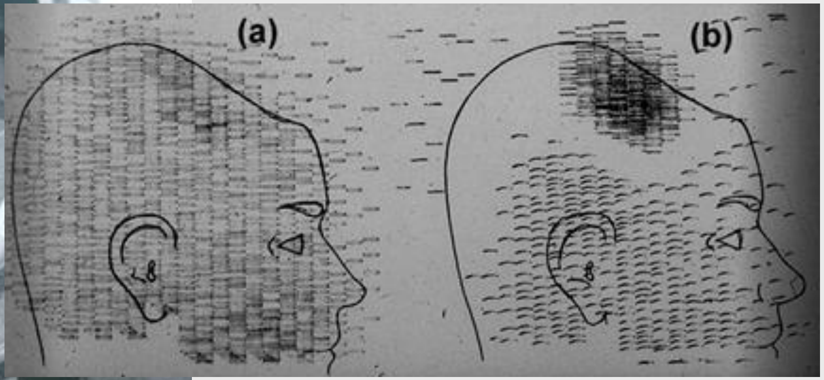

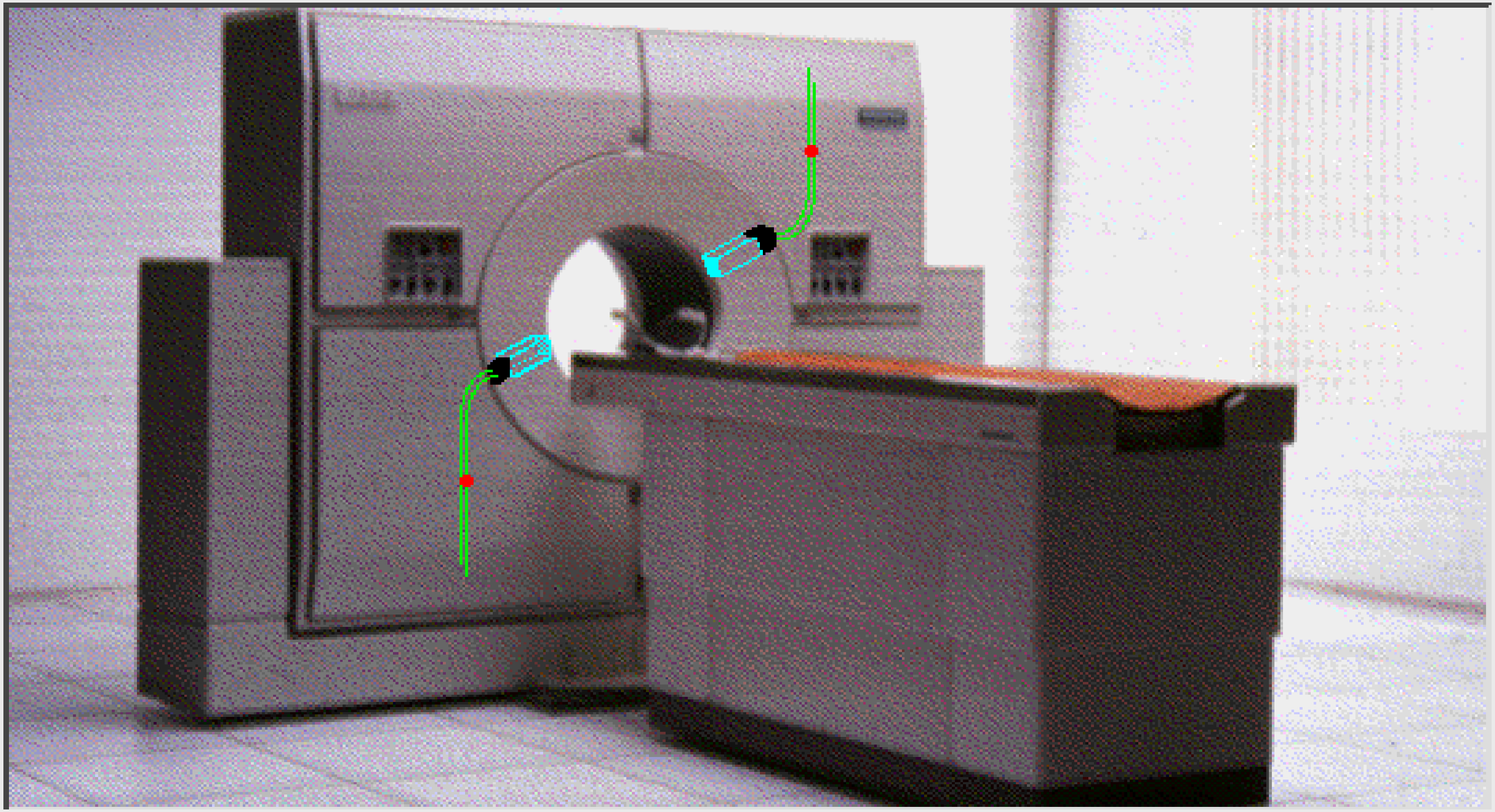

Preclinical Imaging

Small Animal Imaging Suite

Control room
Separated from scanners

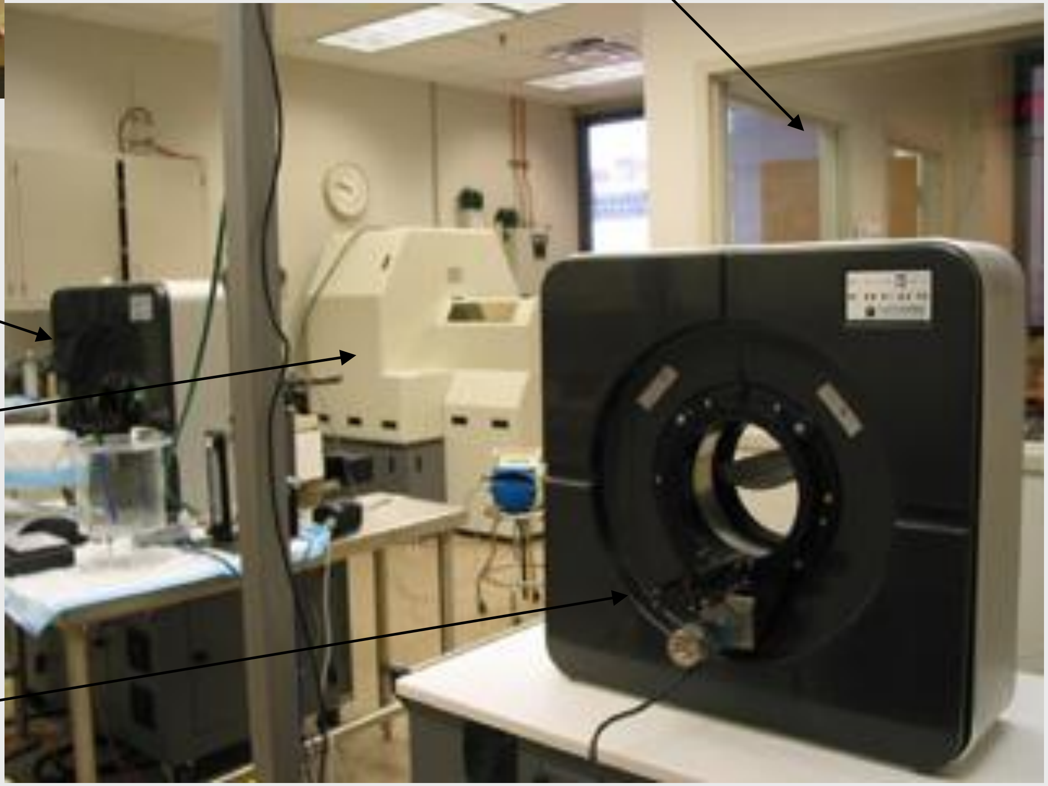

microPET Focus

microCT

microPET Focus

Production of Positron Emitters

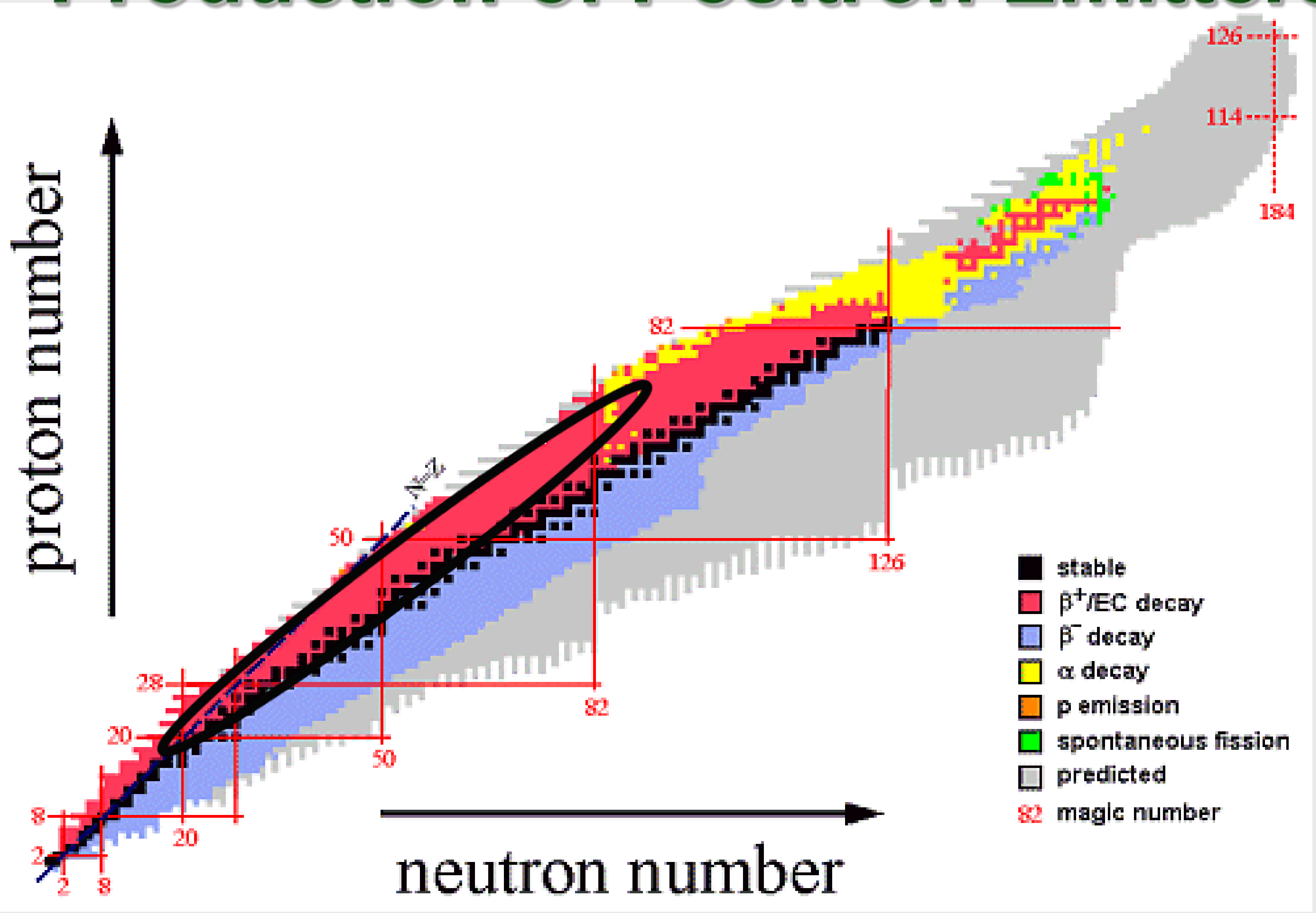

Production of PET isotopes

- β+ isotopes are proton rich
- For use in imaging we typically would like short lived isotopes (minutes to hours)
- Produced by proton induced reactions: (p,n), (p,α), (p,2n)……

Cyclotrons

- Cyclic or repetitive application of force
- Allows small force to be used many times
- Smaller device
- Higher power

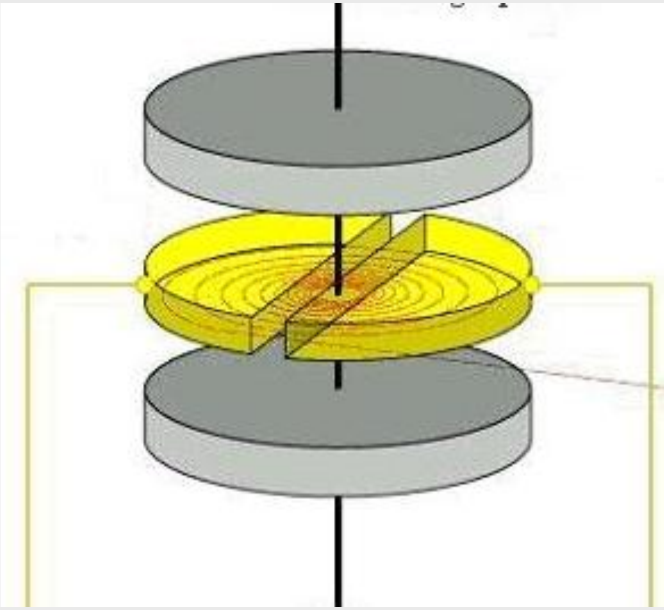

Medical Cyclotrons

- 11-24 MeV protons
- 10 – 500 µA
- Several hundred in operation in the US

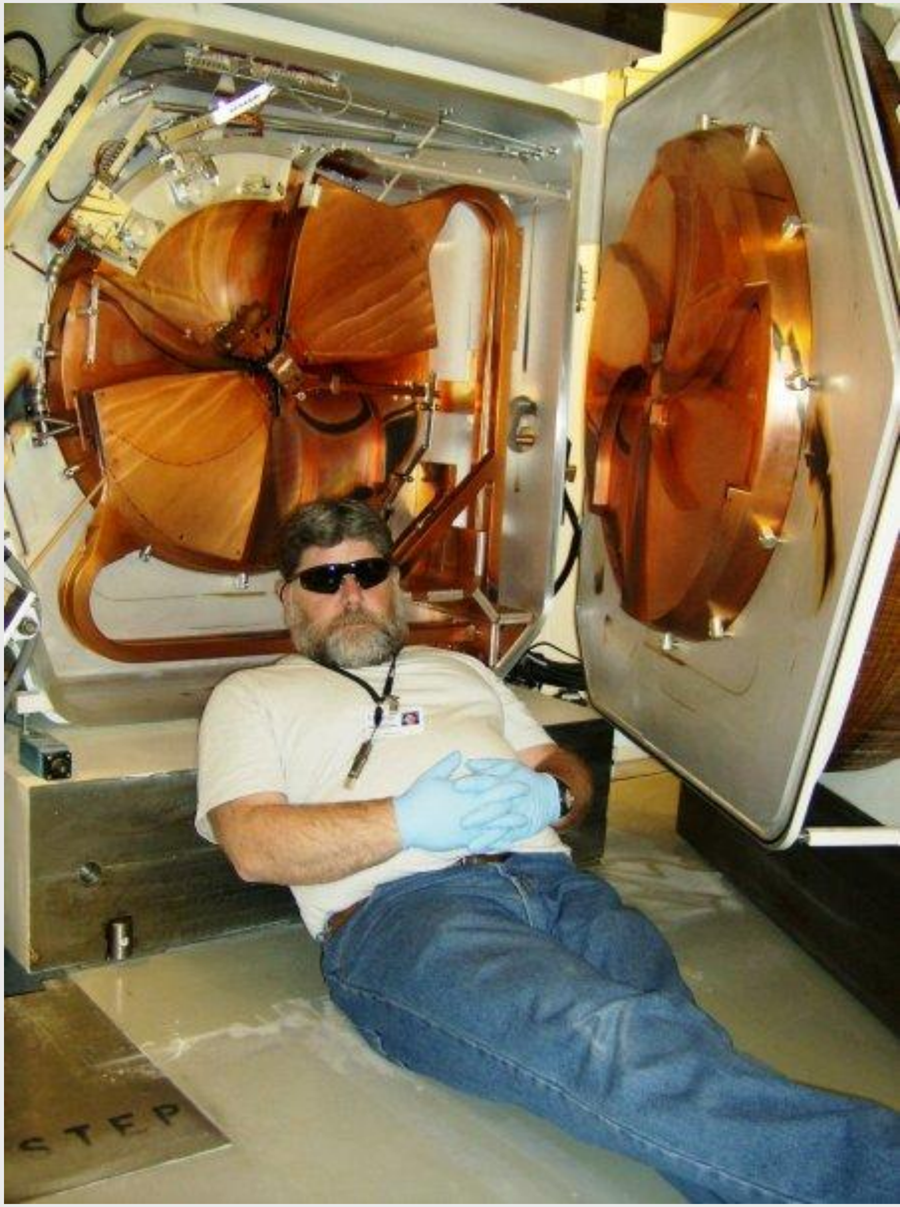

Targetry for cyclotron-produced radionuclides

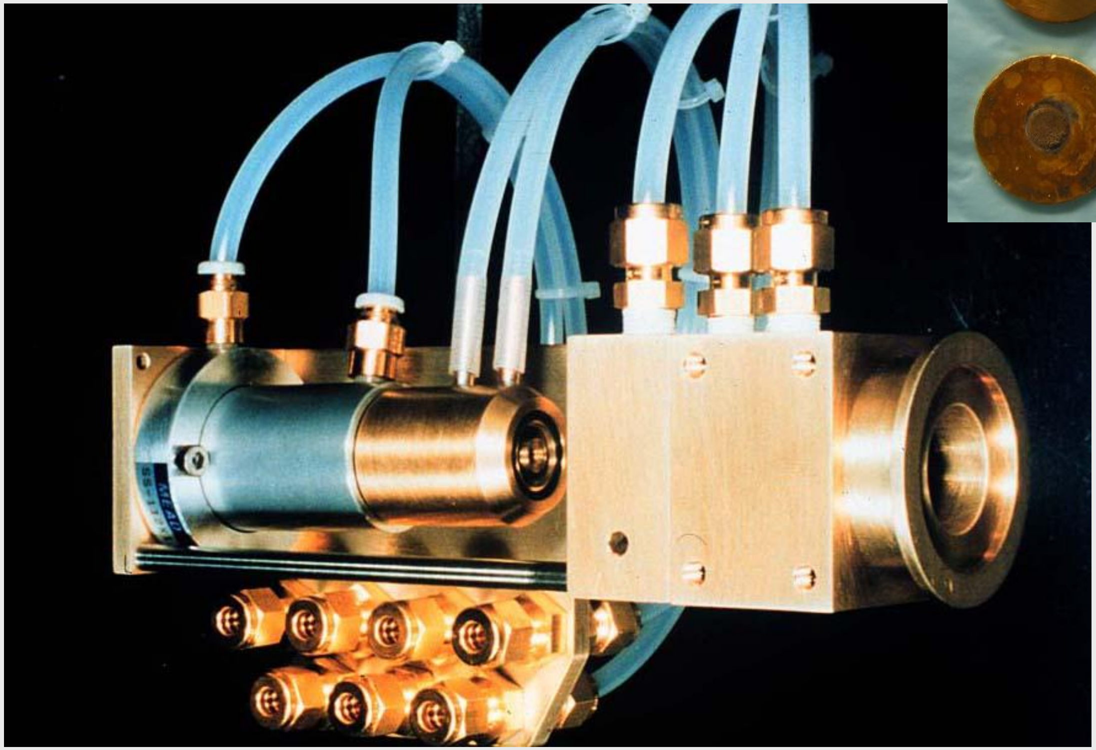

CS-15 Cyclotron and Target Stations

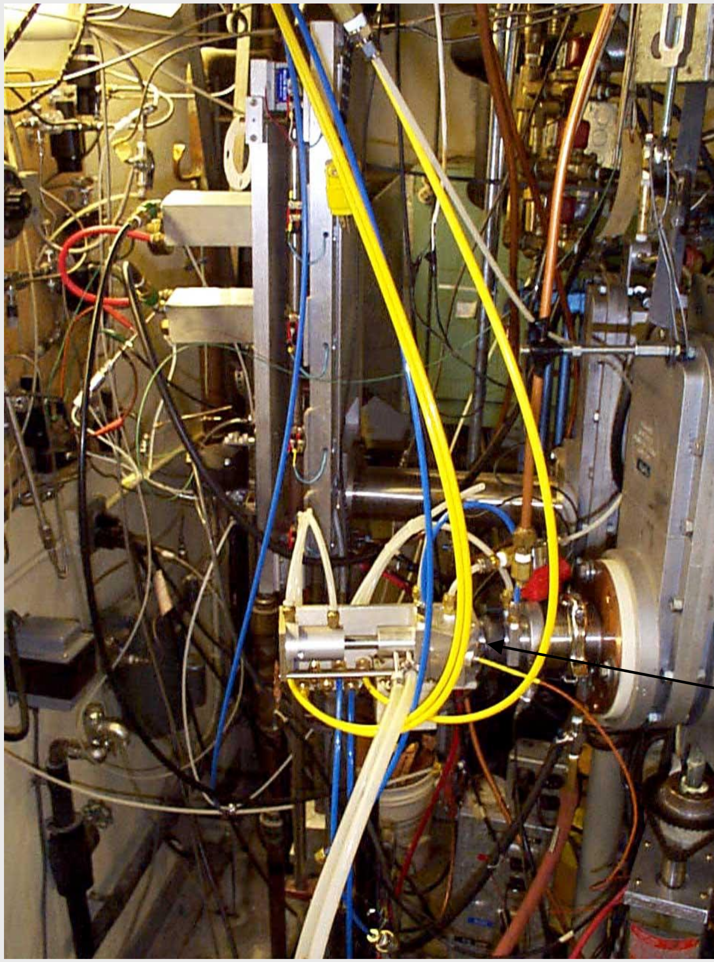

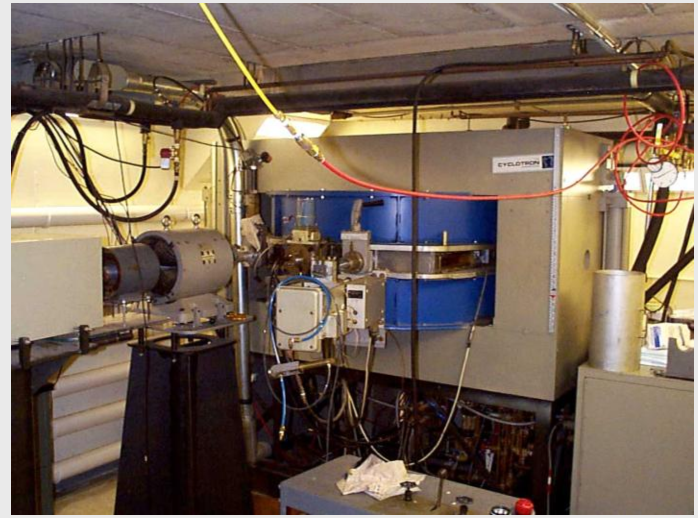

Isotopes……

$^{14}N(p,\alpha)^{11}C$ $t_{1/2}$ = 20.3 min.

$^{18}O(p,n)^{18}F$ $t_{1/2}$ = 109.7 min.

$^{64}Ni(p,n)^{64}Cu$ $t_{1/2}$ = 12.7 h.

Characteristics of non-standard PET Radionuclides

Isotope	Half-life	Decay modes/ %	Max β^+ energy (MeV)	Reaction	Natural abundance of target isotope
^{76}Br	16.2 h	β^+/58.2* EC/41.8	3.98	$^{76}Se(p,n)$	9.1%
^{124}I	4.18 d	β^+/22.0* EC/78.0	2.15	$^{124}Te(p,n)$	4.8%
^{86}Y	14.74 h	β^+/34.0 EC/66.0	3.15	$^{86}Sr(p,n)$	9.9%
^{94m}Tc	52.0 min	β^+/72.0 EC/28.0	2.47	$^{94}Mo(p,n)$	9.3%
^{68}Ga	68 min	β^+/88	1.9	$^{68}Ge/^{68}Ga$ generator	n/a
^{66}Ga	9.49 h	β^+/56.5 EC/43.5	4.15	$^{66}Zn(p,n)$	27.8%
^{60}Cu	23.7 min	β^+/93.0 EC/7.0	3.92	$^{60}Ni(p,n)$	26.1%
^{64}Cu	12.7 h	β^+/17.8* EC/43.8	0.66	$^{64}Ni(p,n)$	1.16%
^{89}Zr	78.5 h	β^-/38.4 β^+/22.8 EC/77.2	0.40	$^{89}Y(p,n)$	100%

*Qaim et al. Radiochimica Acta 2007; 95:67-73

Derenzo Phantom

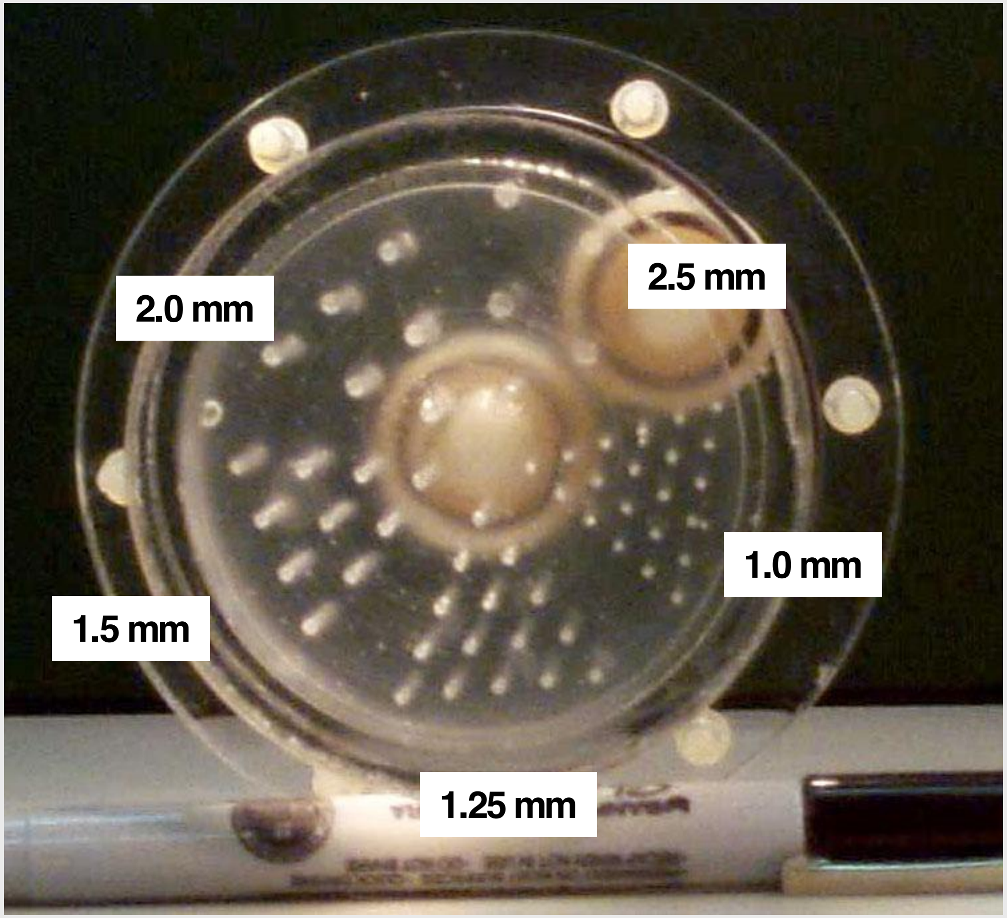

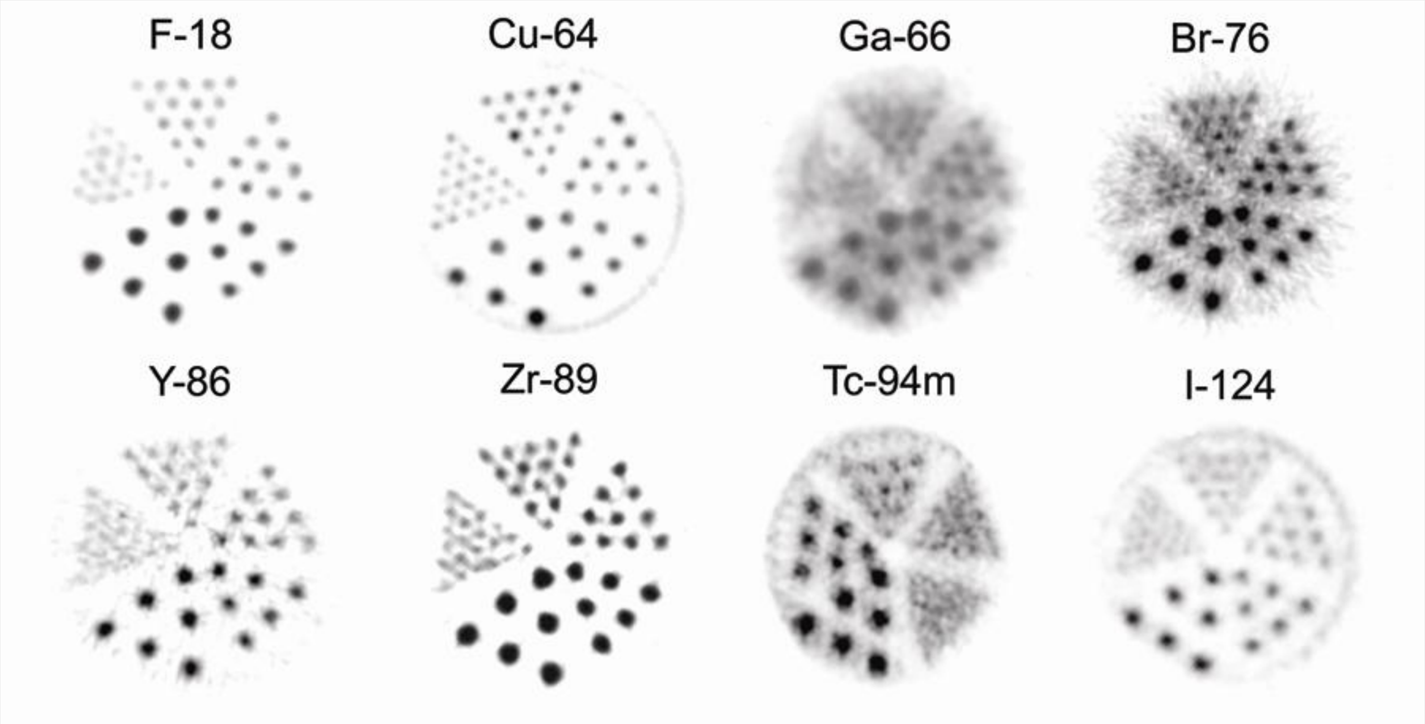

A mini Derenzo phantom filled with various radionuclide imaged on a microPET- Focus scanner (Siemens Medical Systems). This phantom consists of radioactive rods of specified diameter (1.0, 1.25, 1.5, 2.0 and 2.5 mm) separated by four times the diameter. In these images the images were reconstructed utilizing the filtered back projection. It is seen that the nuclides with higher energy positrons and prompt gamma rays produce the image that are degraded compared to those with a single low energy positron (for example, ^{64}Cu and ^{18}F).It is important to note that although this degradation is noted with small animal PET scanners with high resolution (1- 2 mm), this degradation is often not seen with clinical scanners with 4-5 mm resolution. New reconstruction algorithms can also be used to enhance image quality.

PET in Oncology…

- **diagnosis**
  - location and extent of disease
  - general (FDG) or tumour-specific probes
- **prognosis**
  - size, stage, grade of disease
  - proliferation (FLT) and/or hypoxia (EF5, etc)
- **"real-time" therapy evaluation**
  - customizing treatment could increase efficacy, decrease toxicity, and improve economics

FDG:

Glucose

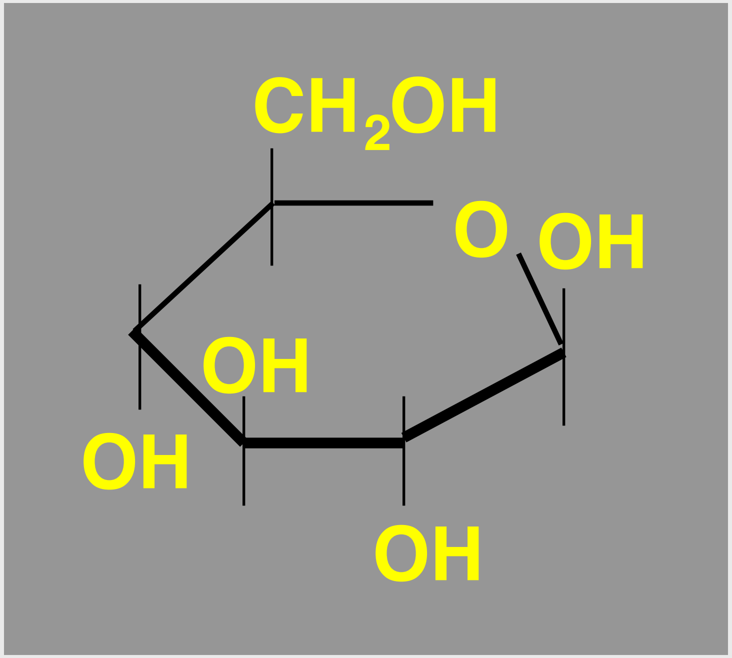

Fluorodeoxyglucose (FDG)

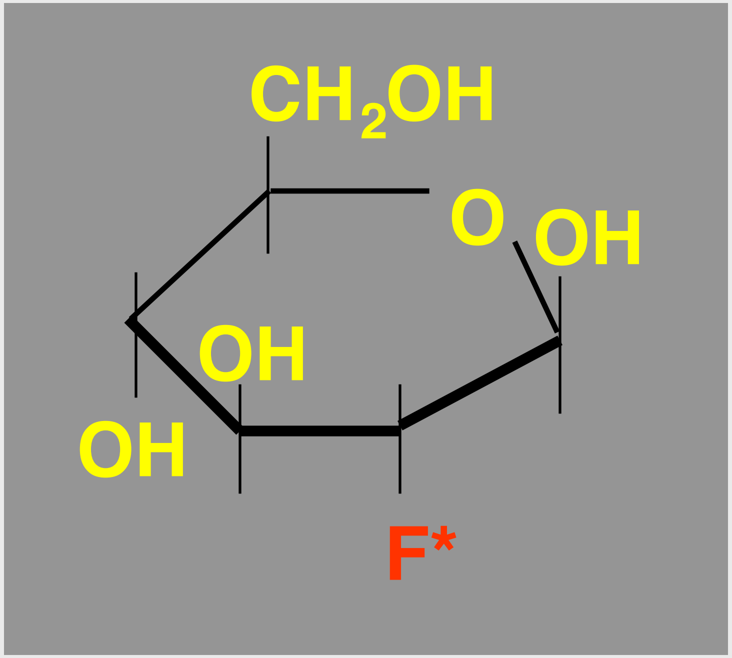

FDG Uptake and Retention

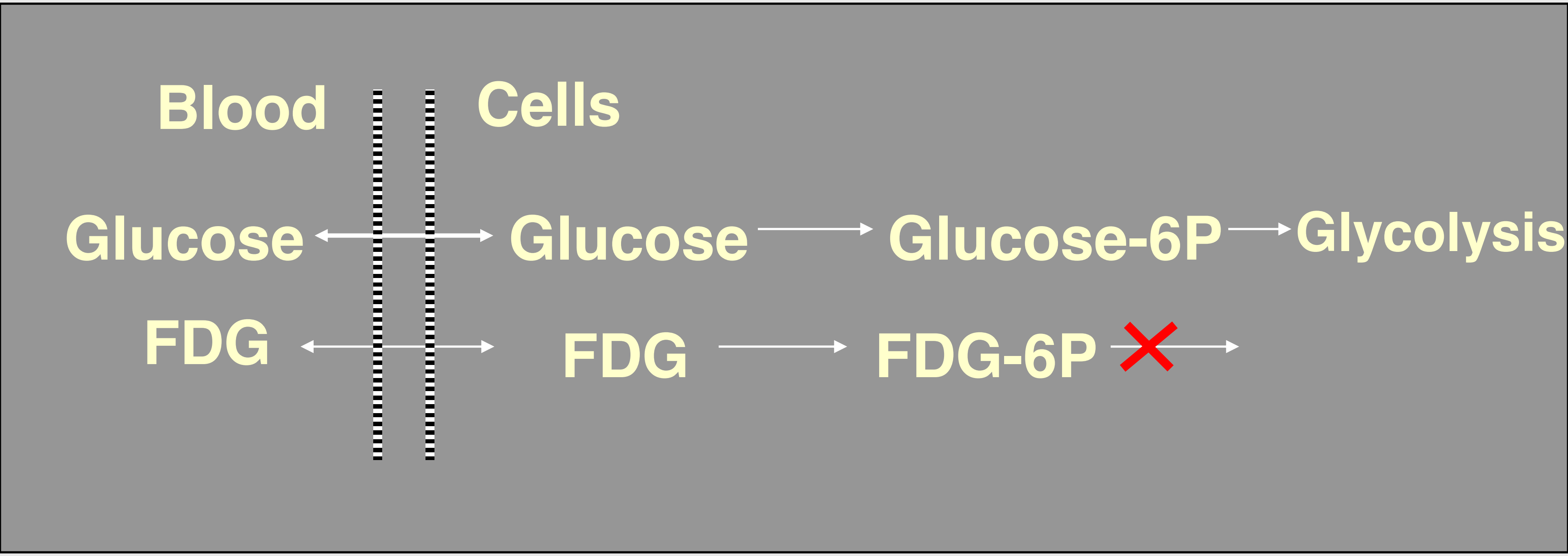

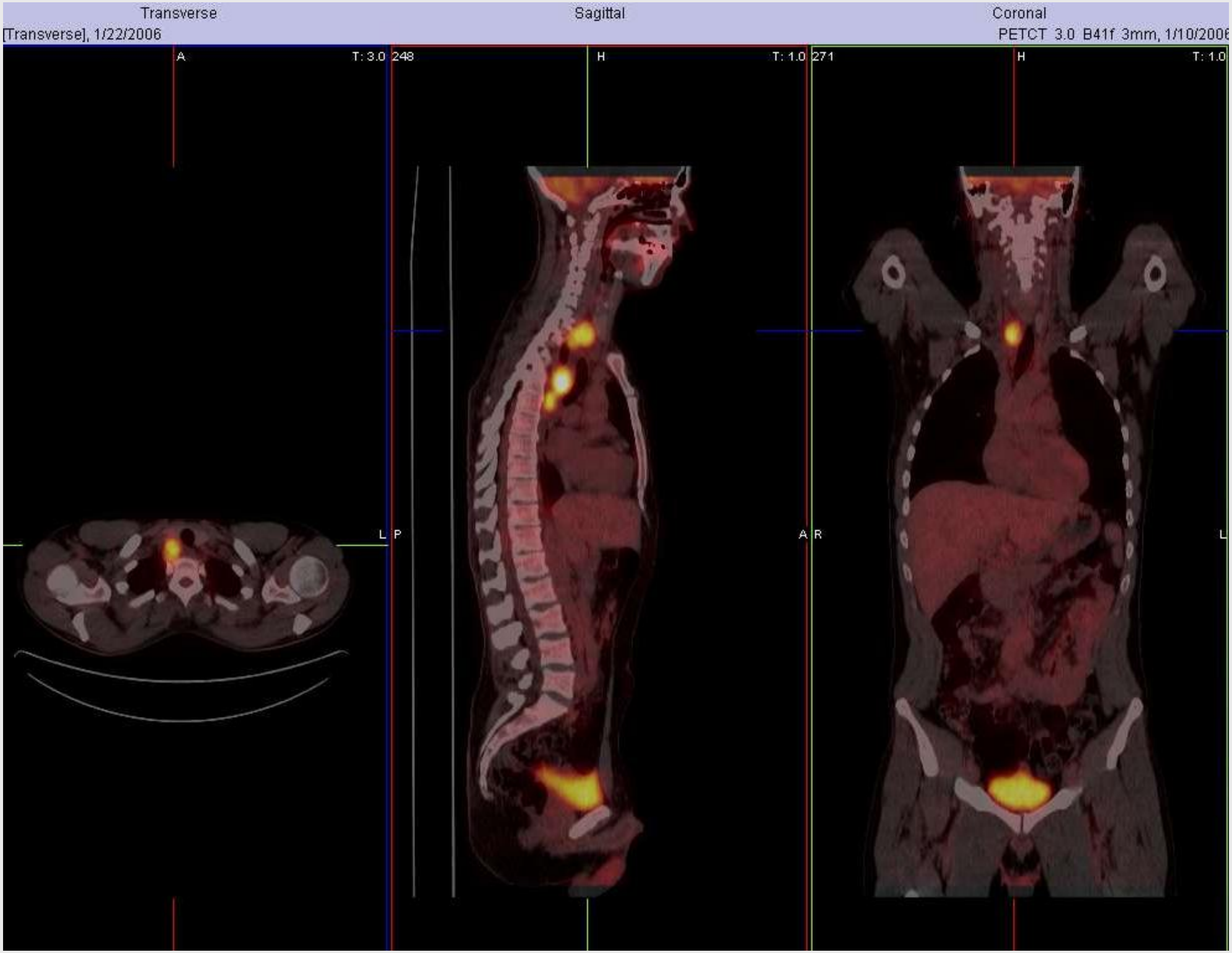
Transverse
Sagittal
Coronal
[Transverse], 1/22/2006
PETCT 3.0 B41f 3mm, 1/10/2006
A
T: 3.0
248
H
T: 1.0
271
H
T: 1.0
L
P
A
R
L

biograph Sensation 16

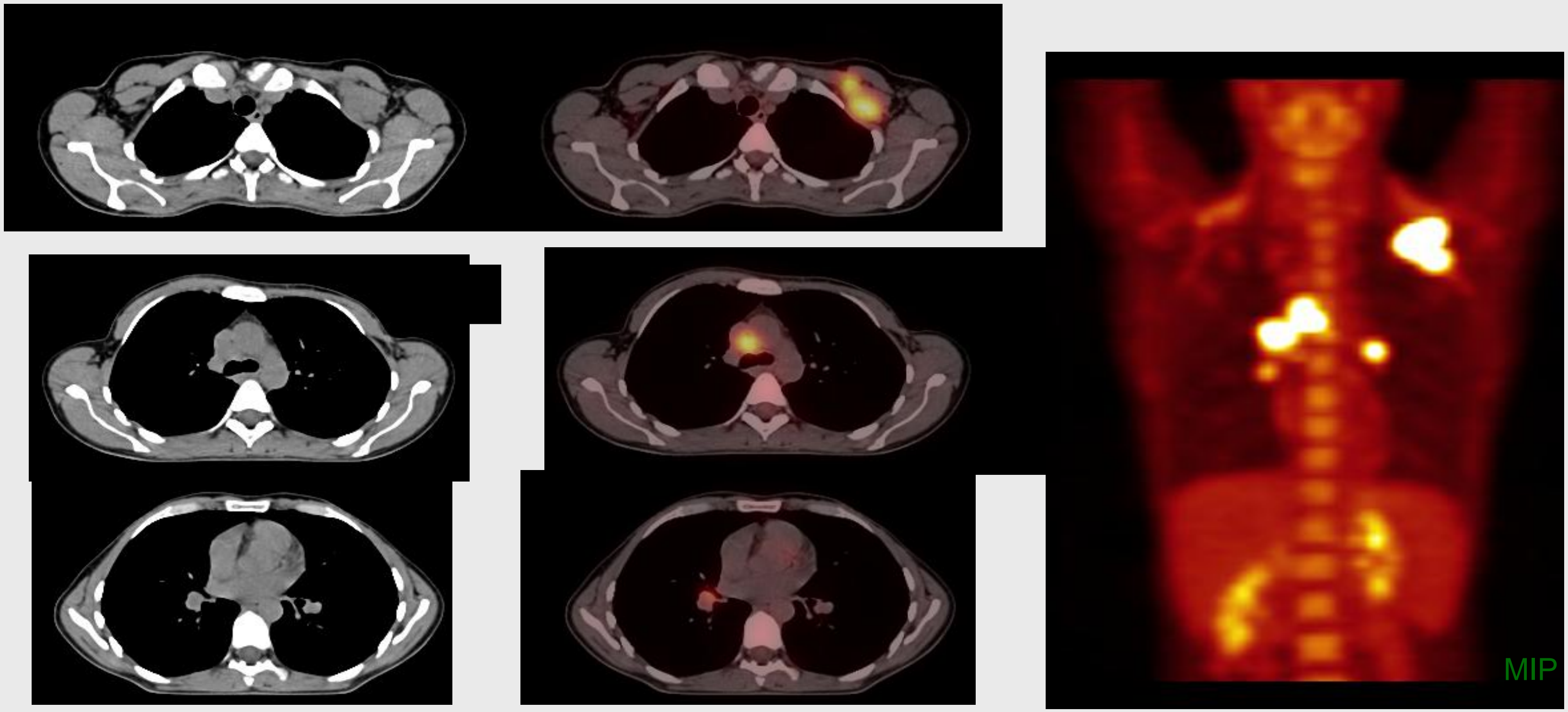

Breast Cancer

37 year old female (53 kg) with history of metastatic breast cancer, for restaging.

biograph Sensation 16 demonstrates multiple areas of increased uptake consistent with metastatic disease, in the mediastinum, bilateral pulmonary hila, left upper lateral chest wall.

Scan protocol: CT 140 mAs, 120 kV, 5 mm slices

PET 400 MBq FDG, 167 min p.i, 5 min/bed, 4+2 beds, 30 min scan time

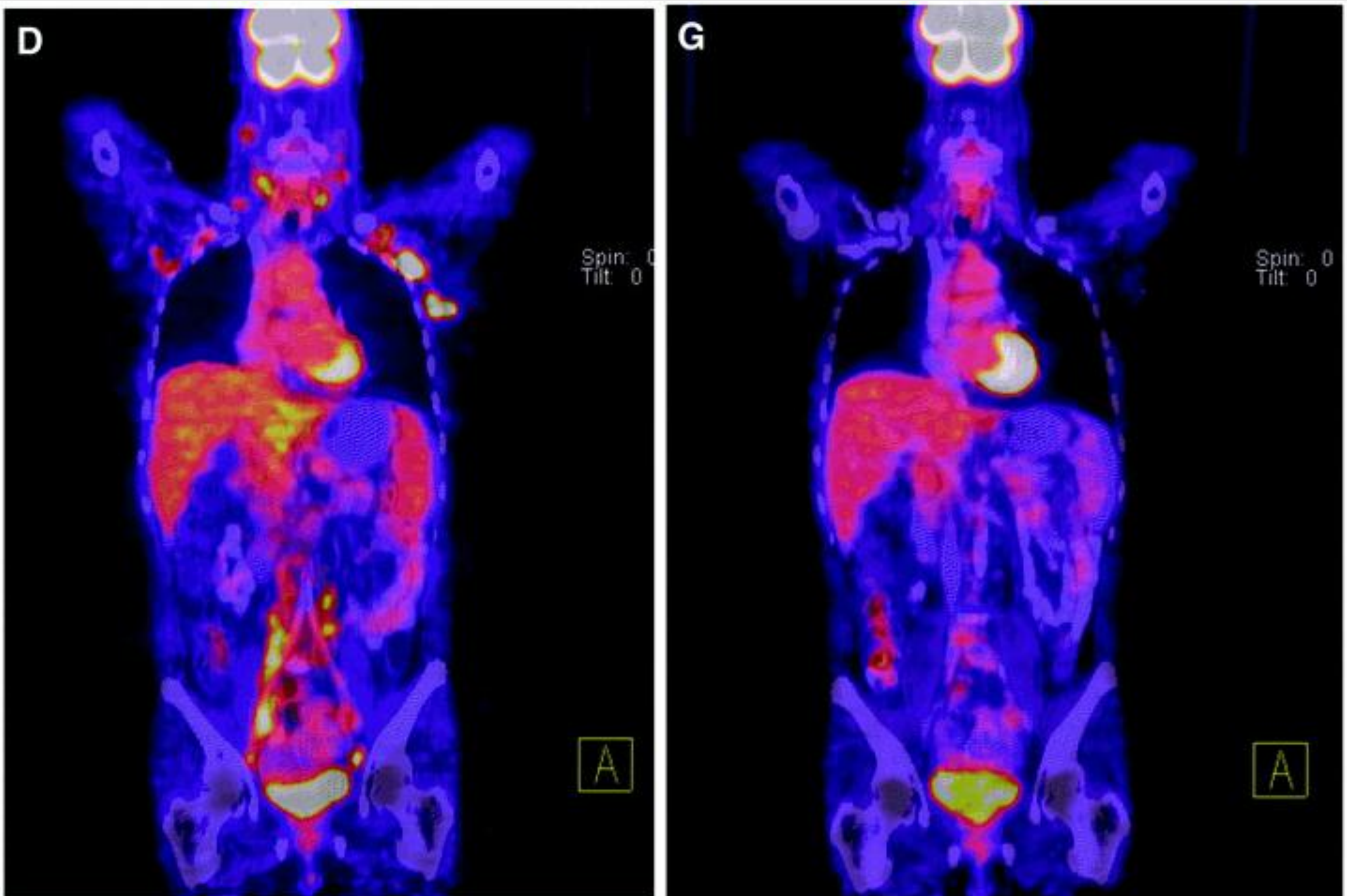

Joyce et al, Clinical Nuclear Medicine, 2005: 30, 564-568

^{18}FDG - micro PET

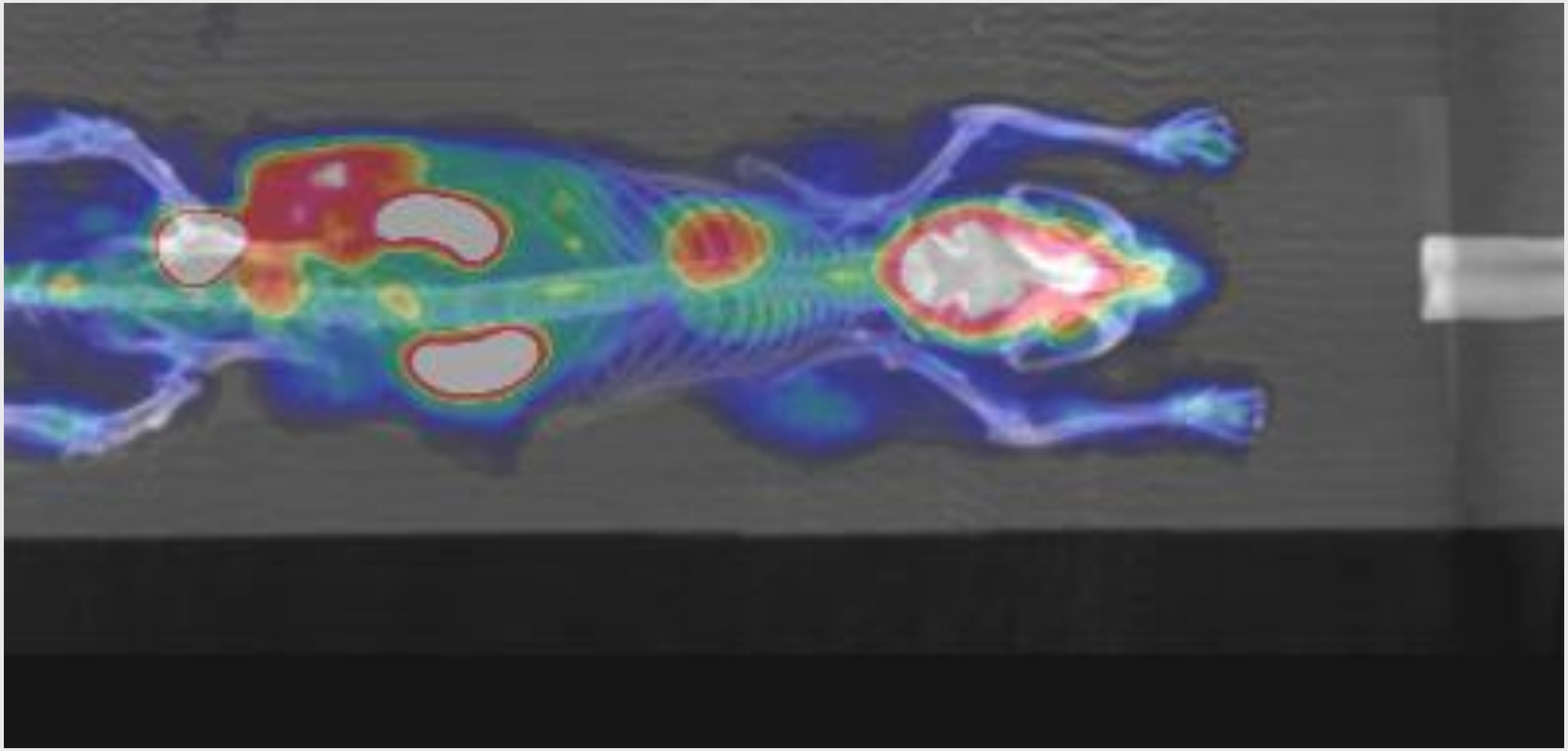

^{64}Cu(ATSM): Why Image Hypoxia?

⇒ Hypoxia influences response to treatment:

(1) Radiotherapy - hypoxic cells are protected from lethal effects of conventional ionizing radiation therapy

(2) Chemotherapy - effect of hypoxia on special genes and drug delivery

⇒ Imaging of hypoxia is required in order to predict response to traditional therapies

⇒ Imaging of hypoxia in the brain, heart and cancer have been explored

PET Imaging Agents – Cu(ATSM)

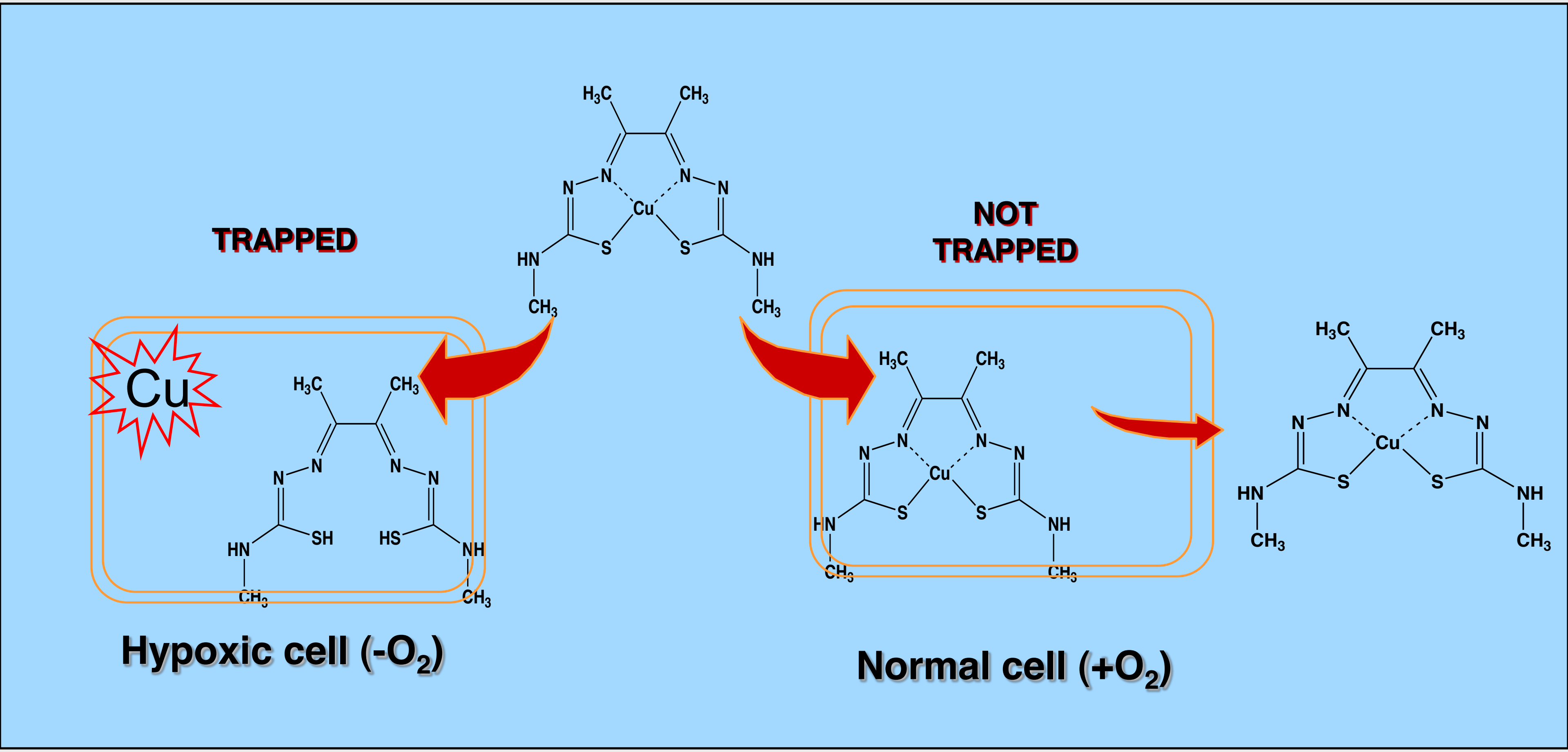

^{64}Cu-ATSM in Cancer of the Uterine Cervix

Responder | Non-Responder

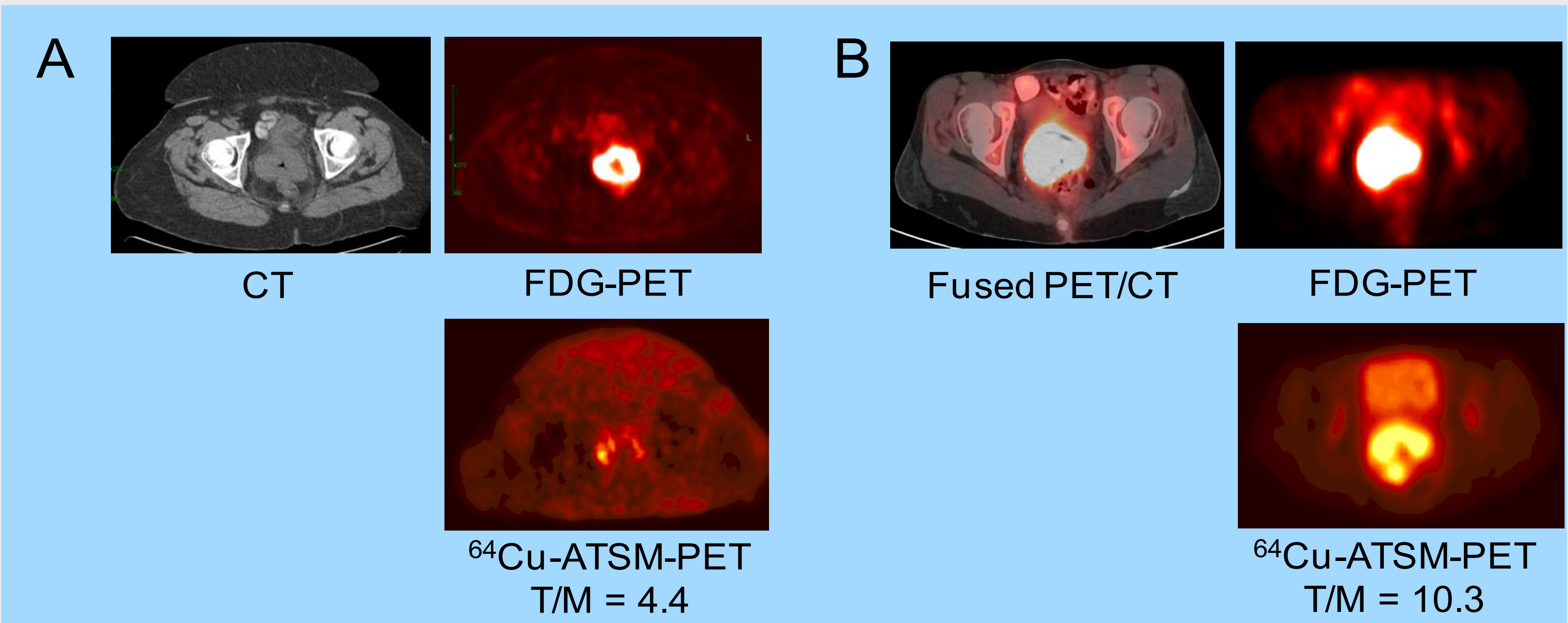

Ca Cervix - Clinical Outcome

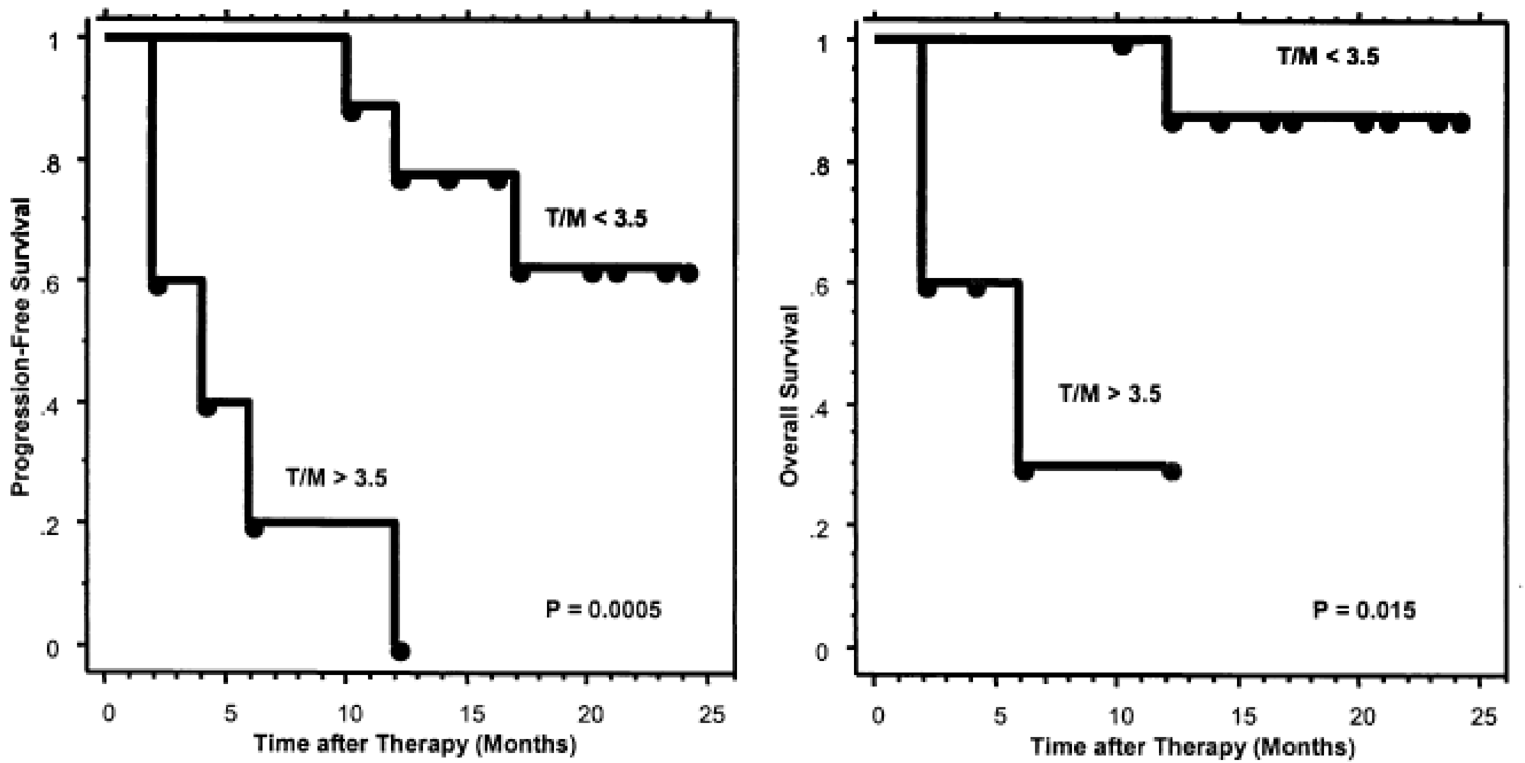

Fig. 2. Progression-free survival and overall survival based on ^{60}Cu-ATSM uptake using Kaplan-Meier method. Patient survival has an inverse relationship with tumor uptake of ^{60}Cu-ATSM assessed by tumor-to-muscle activity ratio (p = 0.0005 and p = 0.015, respectively).

- 5/14 pt's tumors were characterized as hypoxic
- All pts with hypoxic tumors developed recurrent disease
- 6/9 pts with normoxic tumors disease free at end of study

Int. J. Radiation Oncology Biol. Phys., Vol. 55, No. 5, pp. 1233–1238, 2003

Overall Survival Based on ^{60}Cu-ATSM Uptake (T/M) in NSCLC (n=14)

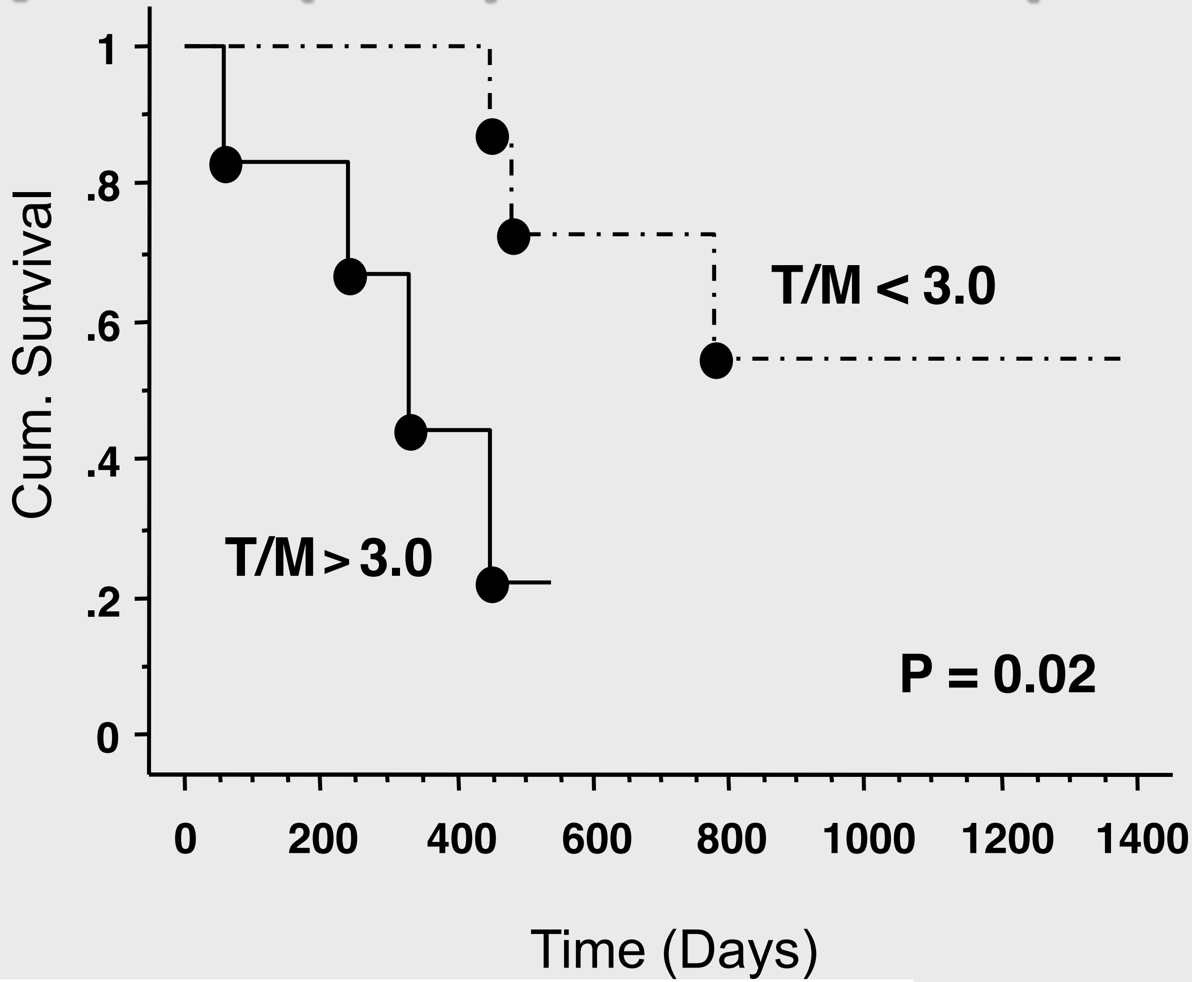

European Journal of Nuclear Medicine and Molecular Imaging Vol. 30, No. 6, June 2003

DOTA-Y3-OC (DOTATOC)

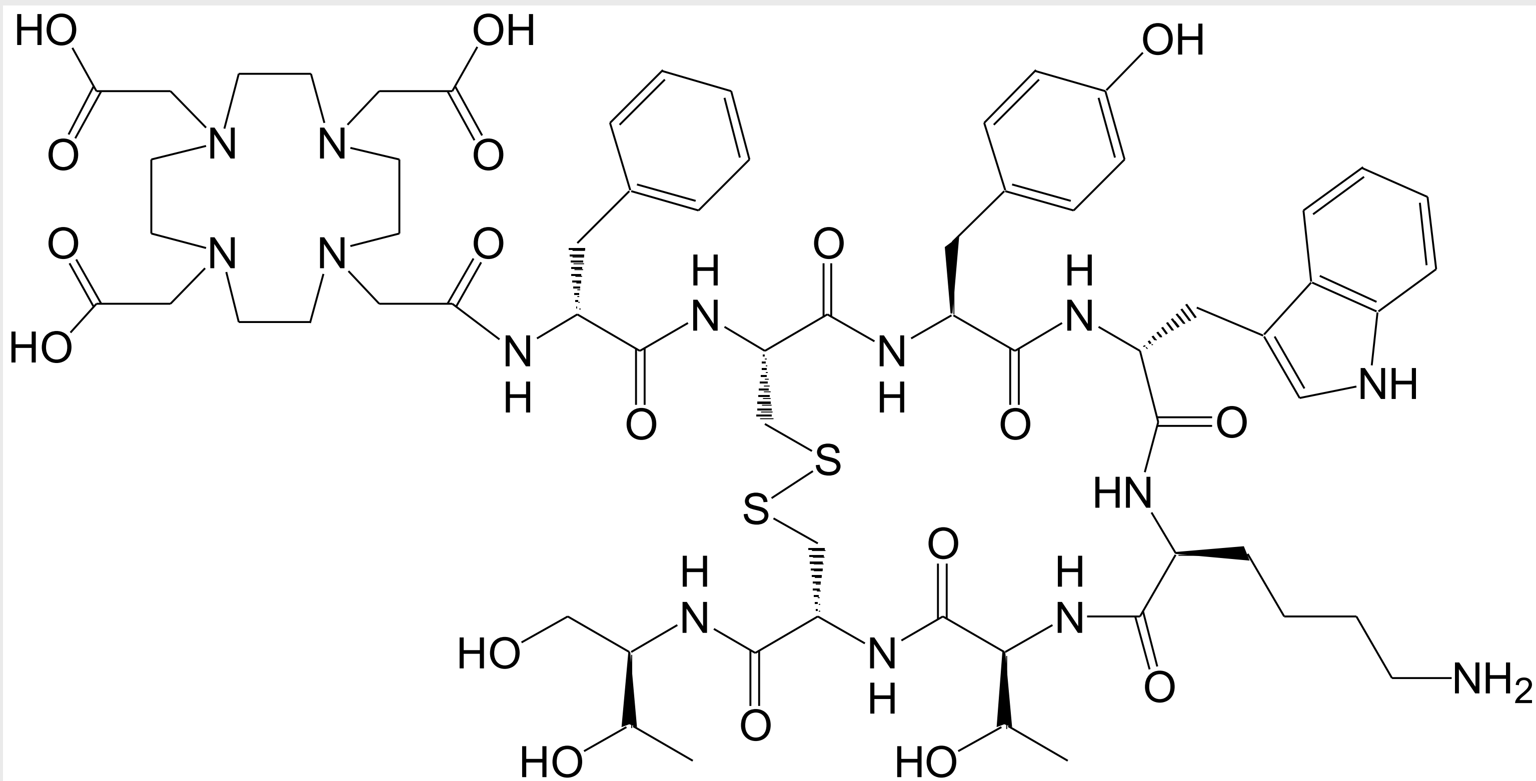

Courtesy of Helmut Maecke, Ph.D.
Univ of Basel, Switzerland

^{68}Ga-DOTA-TOC and PET in Patients with Carcinoid Tumors

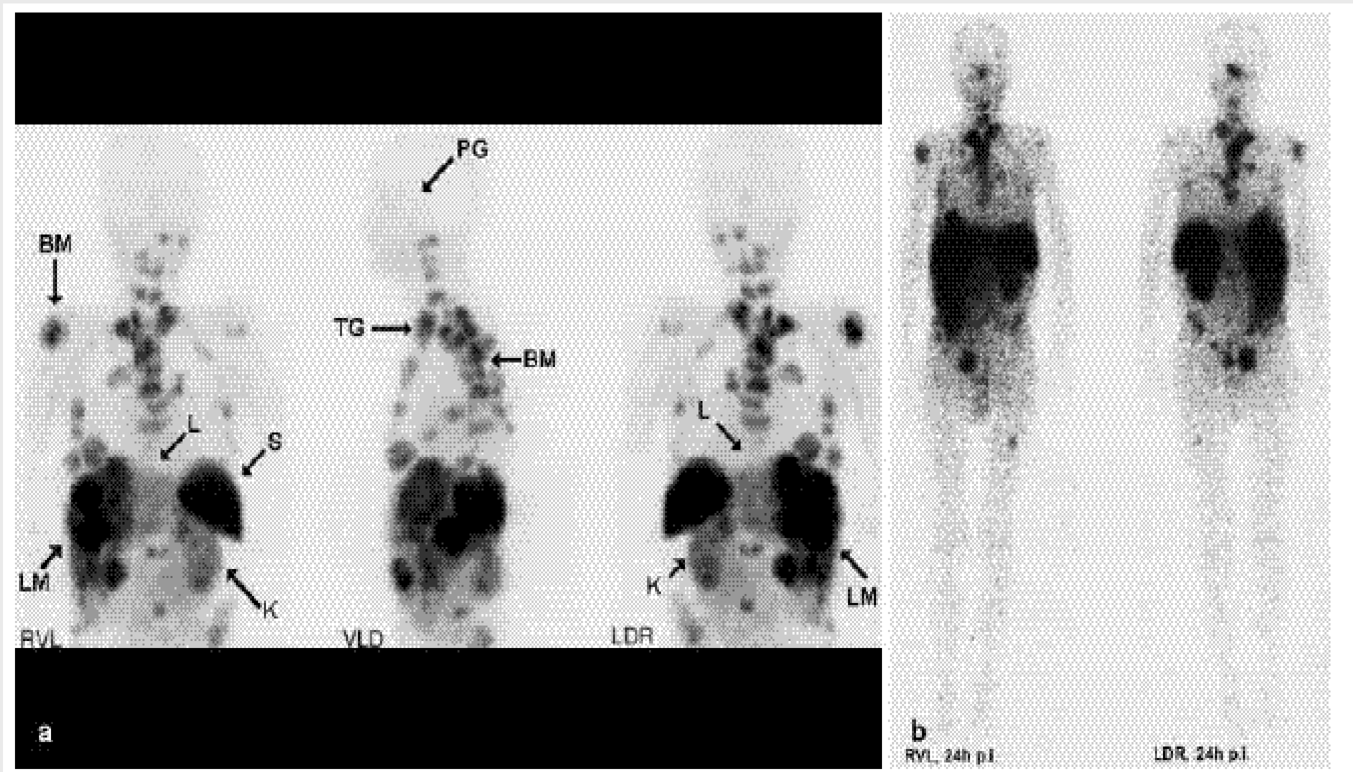

^{68}Ga-DOTA-TOC and PET (left; 90 min post-injection) vs ^{111}In-DTPA-OC gamma scintigraphy (right; 24 h post-injection

Eur J Nucl Med (2001) 28:1751–1757

Case Study

- A 61-year-old man presented with the sudden onset of vision problems of the right eye
- Ophthalmoscopy and MRI were suspicious for a choroidal melanoma
- A subsequent FDG PET showed no FDG accumulation

FDG

Van Riet: Clin Nucl Med, Volume 34(1).January 2009.27-28

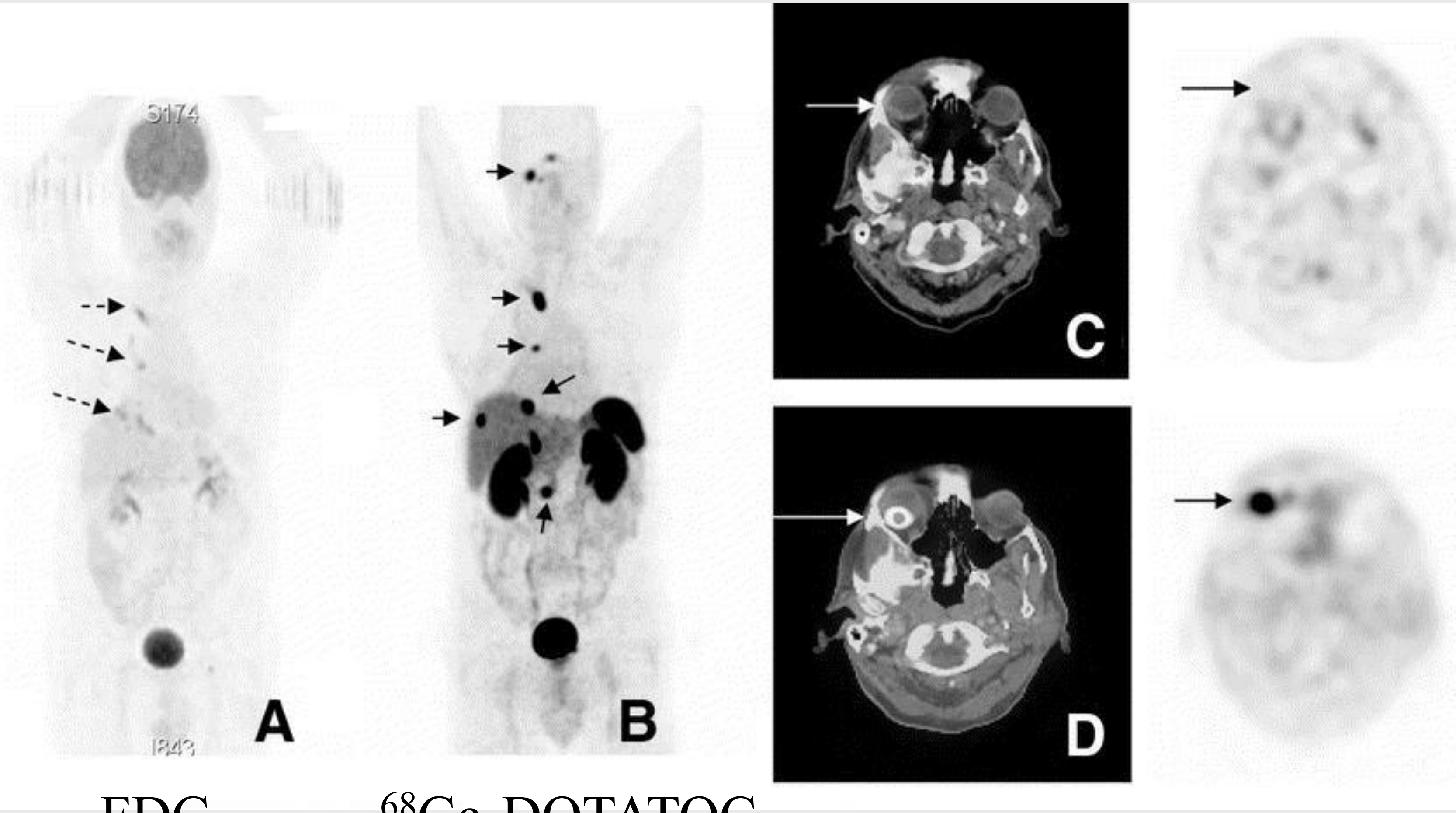

FDG ^{68}Ga-DOTATOC

Van Riet: Clin Nucl Med, Volume 34(1).January 2009.27-28

^{68}Ga-DOTATOC and PET/CT
Metastatic neuroendocrine tumor

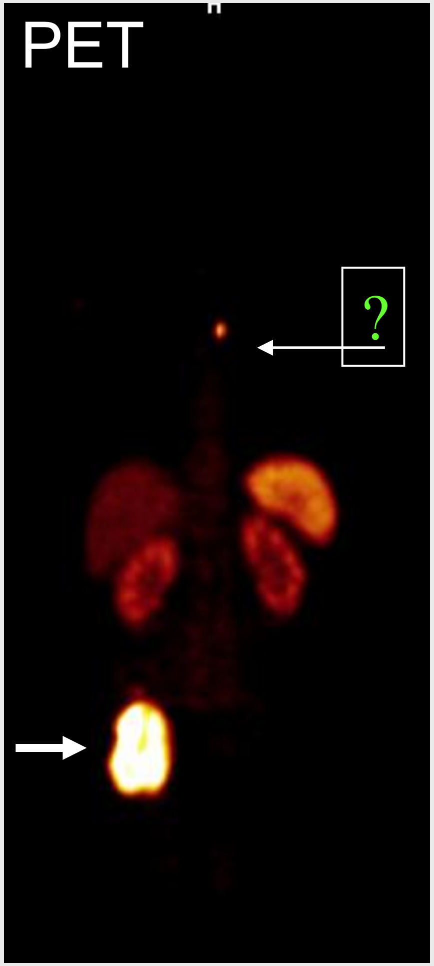

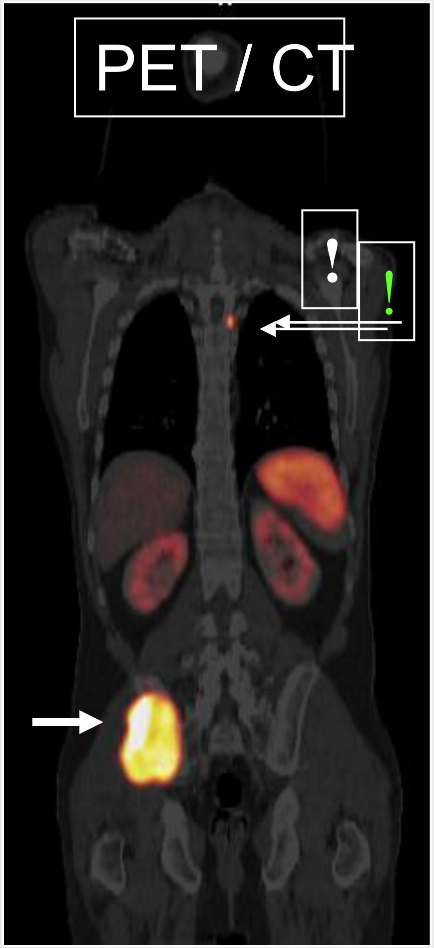

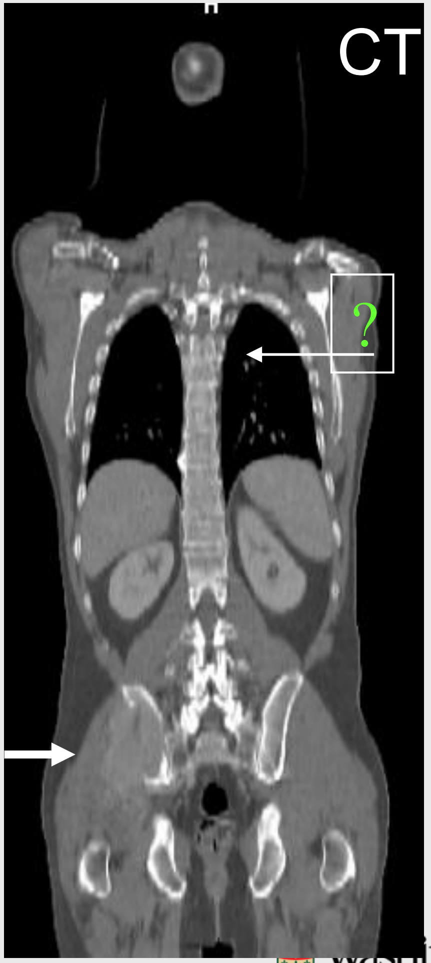

PET + CT

^{89}Zr

- Longer lived metallic radionuclide
- Low positron energy – high quality images
- Produced by $^{89}Y(p,n)^{89}Zr$, ^{89}Y – 100% naturally abundant
- Column chromatography separation

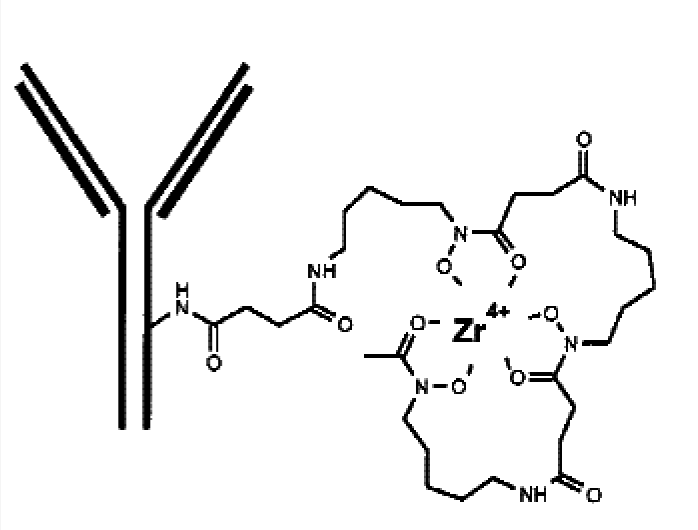

Preclinical ^{89}Zr

[^{89}Zr]-DFO-Herceptin for ImmunoPET (MSKCC)

PET imaging using a HER2/*neu* positive tumors

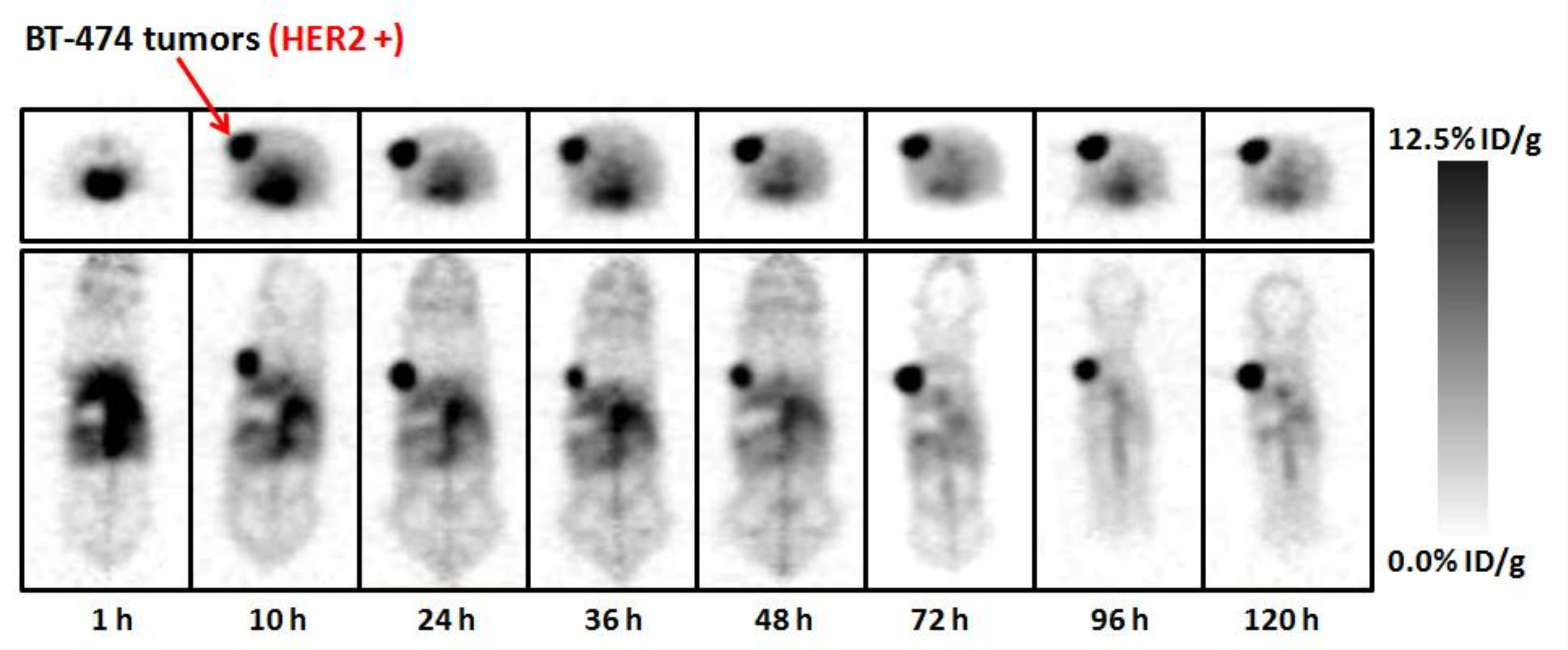

- ImmunoPET images recorded in a female athymic, *nu*/*nu* mouse with sub-cutaneous BT-474 tumors (300 – 450 mm^3)

Clinical ^{89}Zr studies

(Netherlands)

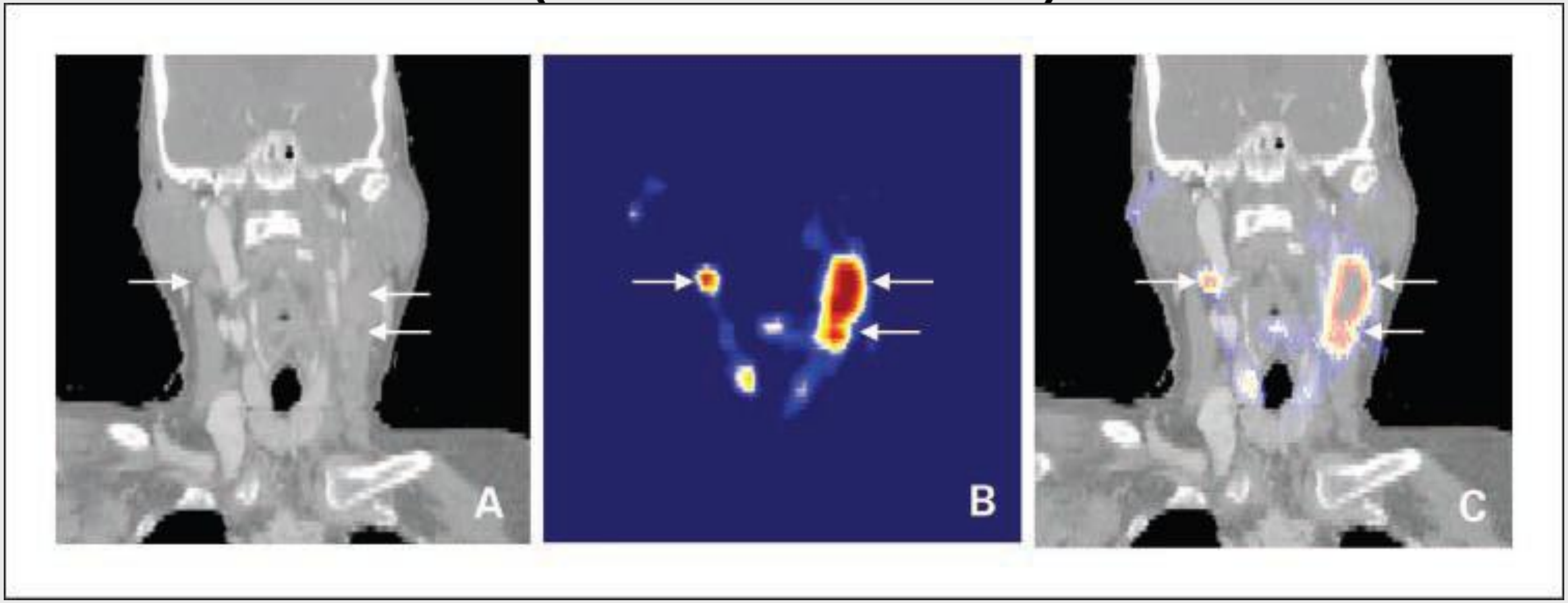

ImmunoPositron Emission Tomography with Zirconium-89-Labeled Chimeric Monoclonal Antibody U36 in the Detection of Lymph Node Metastases in Head and Neck Cancer Patients

- Clin Cancer Res 2006;2133 12(7) April 1, 2006

In other areas:

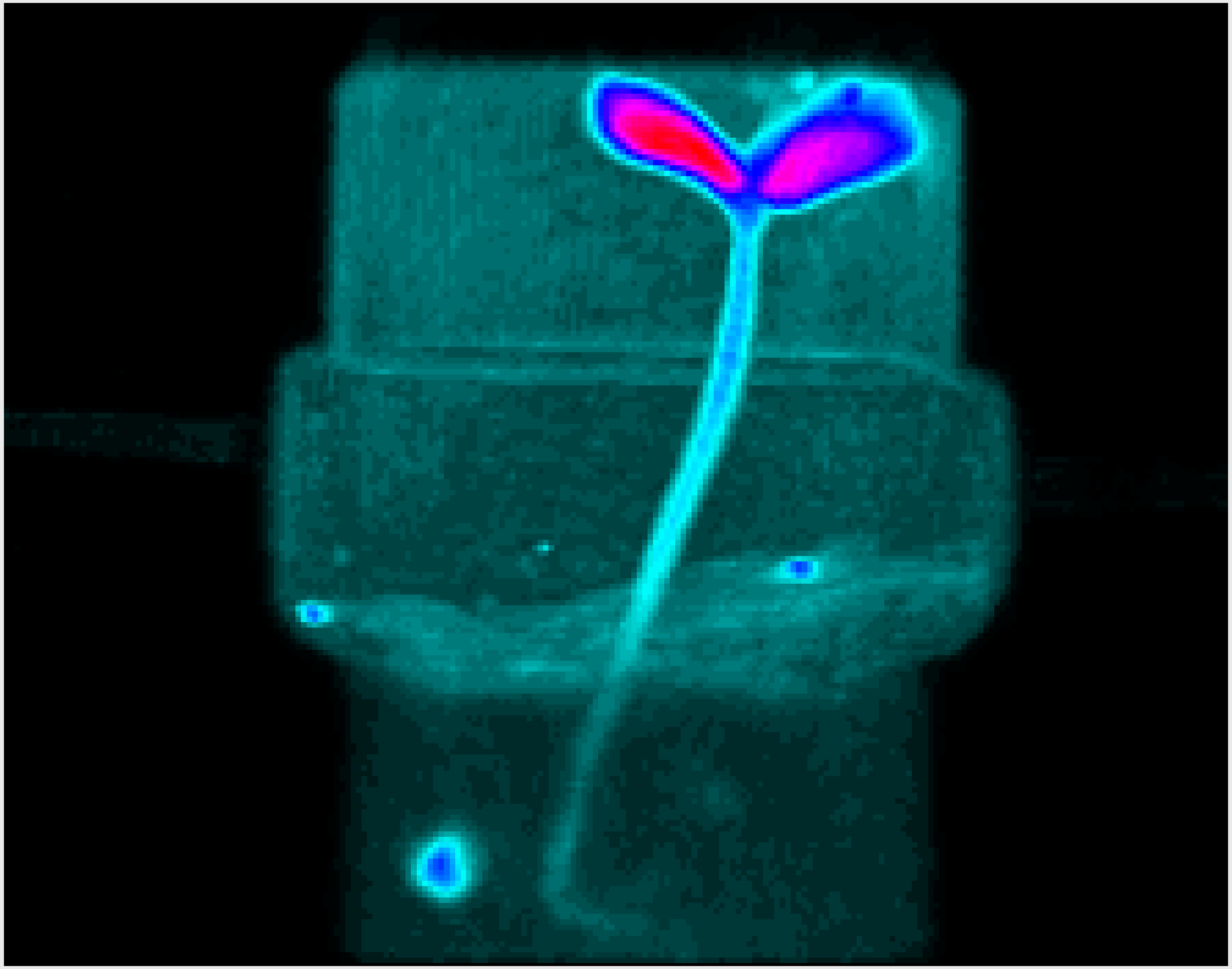

Acknowledgements

Carolyn Anderson, Ph.D.
Jason Lewis, Ph.D.
Jonathan McConathy, M.D., Ph.D.

Lapi Lab Members:

- Oluwatayo Ikotun
- Sandeep Jain
- Efrem Mebrahtu